

Rocking curve and spatial coherence properties of a long X-ray compound refractive lens

V. G. Kohn*

National Research Centre 'Kurchatov Institute', Kurchatov Square 1, 123182 Moscow, Russia.

*Correspondence e-mail: kohnvict@yandex.ru

Received 8 May 2018

Accepted 7 September 2018

Edited by A. Momose, Tohoku University, Japan

Keywords: X-ray focusing; compound refractive lens; rocking curve; computer simulations; recurrent relations; coherence.

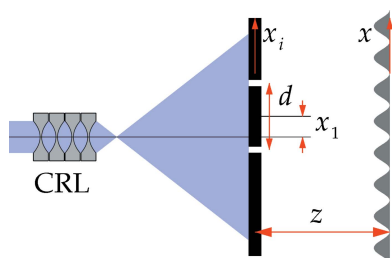
Semi-analytical theory of a long set of X-ray compound refractive lenses (CRLs) based on recurrence relations is developed further. The geometrical aperture, angular divergence of incident radiation and source size were accurately taken into account. Using this theory it is possible to calculate the width of the rocking curve of a long (40.7 cm) Be CRL which coincides with experimental data obtained earlier. By this approach the transverse coherence length for the X-ray beam after passing a set of CRLs of arbitrary complexity has been estimated. It is shown that at the focus this coherence length is equal to a diffraction-limited beam size (beam size in the case of a point source) and has minimal difference with the real beam size.

1. Introduction

X-ray refractive optics were applied for the first time in 1996 (Snigirev *et al.*, 1996), a hundred years after the discovery of X-rays. The reason for this delay was the fact that hard X-ray radiation interacts weakly with matter. The index of refraction deviates from unity with a value of 10^{-6} or smaller. Moreover, the X-ray radiation is absorbed by all materials. It is known that the absorption of X-rays is not strong, and X-rays are used for studying the internal structure of objects. However, this is a severe disadvantage for X-ray refractive optics.

The situation changed in the mid-1990s when third-generation synchrotron radiation (SR) sources became available. These sources generate intensive beams of radiation with photon energy in the range 6–120 keV (wavelength of 0.2–0.01 nm). Today many sources of this kind are under operation. Nevertheless, the first three, namely ESRF (European Synchrotron Radiation Facility) in France, APS (Advanced Photon Source) in USA, and SPring-8 (Super Photon ring) in Japan, allowed many results about the interaction of X-rays with matter to be obtained. Of the new sources, PETRA III in Hamburg, Germany, and X-ray free-electron lasers (XFELs) in general should be noted.

It is important that such sources have undulators with a very small transverse emittance, $\varepsilon = w_s \alpha_0$, where w_s is the transverse size of the source and α_0 is the angular divergence of the beam. As has already been pointed out (ESRF-EBS, 2017), the best values for the undulator radiation at a photon energy of 10 keV are assumed to be $w_s = 5 \mu\text{m}$ and $\alpha_0 = 6 \mu\text{rad}$ in the vertical plane. Correspondingly, the emittance has a value of the order of $\varepsilon = 30 \text{ pm rad}$. A typical source-to-object distance under investigation is 50 m. In this case the transverse size of the free X-ray beam at the object is less than 1 mm. Therefore the relatively small aperture in X-ray refractive lenses becomes comparable with the size of the beam.



It is very useful that the index of refraction for X-rays is less than unity, *i.e.* the phase speed of radiation in matter is larger than the speed of light. Therefore focusing lenses have a bi-concave surface, and the thickness profile of matter has a minimum value in the middle of the aperture. As a result, the decrease in the radiation intensity in the aperture centre due to absorption is weak. Let us consider the complex refractive index $n = 1 - \delta + i\beta$. It was shown by Kohn (2012) that the effectiveness of a lens with a sufficiently large aperture is defined by the parameter $\gamma = \beta/\delta$.

Nevertheless, radiation is absorbed by thick parts of the aperture, and the lens is characterized by an effective aperture, while the focal length is equal to $f = R/2\delta$ for a parallel incident beam and a bi-concave parabolic lens with the curvature radius R at the apex. For a one-dimensional lens the relative intensity of the beam at the focus is equal to γ^{-1} , while the beam transverse size is γ times smaller than the effective aperture.

That is why one has to choose materials for an X-ray lens for which γ has a small value. For the lightest metal Li, γ has the minimum value, but Li is unstable in air and is not widely used. In addition, Li lenses are of poor quality (Pereira *et al.*, 2004). However, Be lenses can be easily manufactured and used (Schroer *et al.*, 2002); today such lenses are produced by B. Lengeler from the Aachen University in Germany.

Let A be the geometrical aperture of a lens (see Fig. 1). The most interesting pairs of parameters (R, A) for the created Be lenses are as follows (in micrometres): (50, 450), (100, 632), (200, 894), as reported by Lengeler (2010). Since the focal length for one such lens is very large, in real experiments a compound refractive lens (CRL) is used. It consists of an array of elements that are positioned in a holder that provides their correct position relative to the beam.

We note that CRLs of other low- Z materials like Al and polymers have been produced as well and used in experiments (see, for example, Snigirev *et al.*, 1998; Ohishi *et al.*, 2001). A CRL made from N elements has a focal length $f = R/2N\delta$ in the thin-lens approximation. In spite of the large length of a CRL (much larger than the aperture size), the CRL can be considered as a thin lens with an effective curvature radius $R_0 = R/N$, if the focal length is several times larger than the CRL length along the beam (Kohn, 2003). Today, Be CRLs are widely used for both focusing and imaging. They are basic elements of a high-resolution X-ray microscope (Bosak *et al.*, 2010; Snigireva *et al.*, 2011), allowing photonic crystals to be imaged with a resolution of <50 nm.

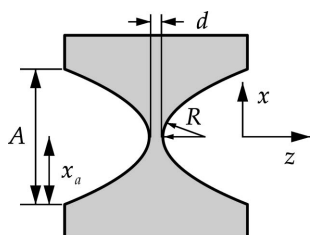


Figure 1
Parameters of one chip of the CRL.

However, it is easy to create a CRL of a length larger than the focal length in the thin-lens approximation. The theory for such a CRL was first developed by Kohn (2002, 2003) under the assumption that the elements of the CRL are packed closely. Such an assumption allows the development of an analytical expression for a propagator of the long CRL as a function which describes the wavefield at the exit surface of the CRL for a point source at the entrance surface. Later the semi-analytical theory was developed (Kohn, 2009a,b, 2012) for a long CRL system which is valid for arbitrary configuration of CRLs in space.

This work presents a further development of that approach. There are three points which have been improved. The first point is the angular divergence of the incident beam. The second point is the problem of accounting for the geometrical aperture of a CRL. The third point is an accurate account of the source size. In this paper two new results are presented. The first result is that the semi-analytical theory allows the full width at half-maximum (FWHM) of the rocking curve of a CRL to be calculated which coincides with the experimental results obtained in the work of Snigireva *et al.* (2004). The second result is the possibility to calculate coherence properties of the beam behind the long system of CRLs at any distance from the CRL. In both cases the calculations are simple and quick and they are performed using an online computer program (Kohn, 2018).

2. General equations

Let us consider an experimental setup which includes a set of CRLs with arbitrary distances between them (see Fig. 2). The CRLs are installed in a beam path along the z -axis. The full set-up is shown in Fig. 3(a). SR from the source becomes monochromatic with good accuracy by means of a monochromator (not shown). The monochromator does not change the direction of the X-rays. The time of observation is much longer than the duration of the X-ray pulses. Under these conditions it is necessary to consider as coherent only monochromatic harmonics of the radiation (Afanas'ev & Kon, 1977). In a first step we calculate the intensity of the monochromatic radiation at the detector. In a second step this intensity has to be integrated over frequency with a radiation spectrum as a weight function to take into account polychromaticity.

We note that this is not the case for SR because the radiation spectrum after the monochromator is very narrow and the SR can be considered as monochromatic. In the case of XFELs the problem of polychromaticity was considered by Kohn (2012).

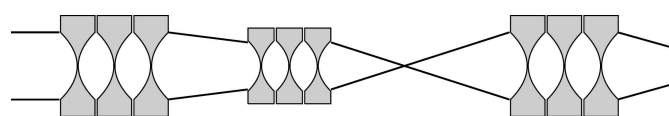


Figure 2
Scheme of several CRLs in the beam path.

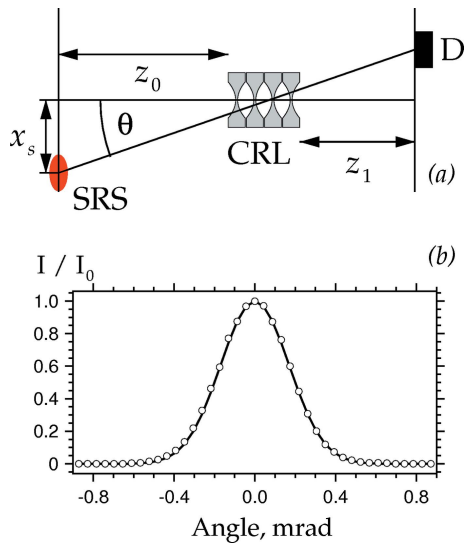


Figure 3
 (a) Scheme showing that a shifted source is equivalent to a rotating CRL. Here, SRS is the synchrotron radiation source and D is the detector. A new optical axis makes an angle θ with the old axis. In reality $x_s \ll z_0$.
 (b) The experimental rocking curve (markers) is taken from the work of Snigireva *et al.* (2004) and the theoretical rocking curve (solid line) is from this work.

We can neglect the monochromator because it does not influence the intensity distribution of monochromatic radiation at the detector. For this reason each point at the source transverse section has to be considered independently. In a first step we consider the completely coherent point source and use Maxwell’s equation for calculating the electric field of radiation during its propagation from the source to the detector through an optical system. In a second step the intensity of radiation at the detector has to be integrated over all points of the source transverse size taking into account the intensity distribution (density of radiation) inside the source transverse size.

Such a model is completely sufficient in the case of X-rays. It allows one to calculate theoretical results which fully coincide with the experimental results obtained with a third-generation SR source (Kohn *et al.*, 2000, 2001). We note that in some works (for example, Singer & Vartanyants, 2014) the Gaussian Schell-model source and the function of spectral degree of coherence are considered according to the general theory of coherence (Mandel & Wolf, 1995). However, this approach is rather complicated, especially in the case of a long CRL system.

We consider first the one-dimensional CRL in the plane (x, z) . Let us assume that the electric field of the incident radiation from a point at the source position with the transverse coordinate x_0 can be described in front of the first CRL by the function

$$E_0(x) = (i\lambda)^{1/2} P(x - x_0, z_{0c}), \quad (1)$$

where

$$P(x, z) = \frac{1}{(i\lambda z)^{1/2}} \exp\left(i\pi \frac{x^2}{\lambda z}\right) \quad (2)$$

is the Fresnel propagator as a transverse part of the spherical wave in the paraxial approximation,

$$z_{0c} = z_0 \left(1 + i \frac{\sigma_r}{z_0}\right)^{-1}, \quad \sigma_r = e_1^2 \frac{\lambda}{\alpha_0^2}. \quad (3)$$

Here z_0 is the distance from the source to the beginning of the first CRL (see Fig. 3), λ is the radiation wavelength, α_0 is the angular divergence of the beam due to relativistic phenomena, and $e_1 = (2 \ln 2/\pi)^{1/2} = 0.6643$.

It is easy to verify that the intensity $I_0 = |E_0|^2$ of such a field at distance z_0 is equal to

$$I_0(x) = \frac{1}{z_0} \exp\left(-\ln 2 \frac{x^2}{x_r^2}\right), \quad x_r = \frac{z_0 \alpha_0}{2}. \quad (4)$$

One can see that $z_0 I_0(x_r) = 0.5$. Here and below we use the full width at half-maximum (FWHM) as a measure of the width for Gaussian functions. Thus the parameter σ_r allows one to take into account phenomenologically the finite angular divergence of the beam.

The CRL is an array of elemental bi-concave lenses (chips) with a relatively large curvature radius R and a large focal distance f . We can consider each chip as a thin lens and describe it by the transmission function (Kohn *et al.*, 2003)

$$T(x, f_c) = \exp\left(-i\pi \frac{x^2}{\lambda f_c}\right), \quad (5)$$

where

$$f_c = \frac{f}{1 - i\gamma}, \quad f = \frac{R}{2\delta}, \quad \gamma = \frac{\beta}{\delta}. \quad (6)$$

This function is applied for all chips of the CRL except the first one. For the first chip the function has to be modified with the aim of taking into account the geometrical aperture of the CRL.

We assume that there is a slit in front of the CRL which absorbs all radiation out of the aperture of size $2x_a$ (see Fig. 1). Therefore the correct expression for the transmission function of the first chip has to be

$$T(x, f_c) = \exp\left(-i\pi \frac{x^2}{\lambda f_c}\right) \theta(x_a - |x|), \quad (7)$$

where $\theta(x)$ is the Heaviside function which equals unity for a positive argument and zero for a negative argument. However, we want to approximately replace the Heaviside function by the Gaussian function with the same integral intensity of the beam in the limit $\gamma = 0$ (transparent lens). Namely, we use the function $\exp[-\pi x^2/(8x_a^2)]$ instead of the function $\theta(x_a - |x|)$ (Kohn, 2017). It is easy to verify that the squared values of these functions give the same integral in the infinite limits. In this approximation the transmission function of the first chip has the form of equation (5) but with a replacement of γ by

$$\gamma_1 = \gamma + \frac{\lambda f}{8x_a^2}. \quad (8)$$

Let us assume that we know the electric field $E_n(x)$ in front of the n th chip. Then the electric field in front of the $(n + 1)$ th chip can be calculated as

$$E_{n+1}(x) = \int dx_1 P(x - x_1, z) T(x_1, f_c) E_n(x_1), \quad (9)$$

where z is the distance between chips. In reality a chip has a thickness $p = d + x_a^2/R$, where d is the thickness of a thin layer of material between two surfaces of the bi-concave lens (see Fig. 1). In the approximation of phase contrast imaging the object (the chip in our case) is considered as being very thin with the same phase shift and absorption, but the distance z has to be greater than p . It can be much greater in a transition from the last chip of one CRL to the first chip of another CRL or to a detector.

In the works by Kohn (2009a,b, 2012) the theorem was formulated that if the electric field in front of the n th cheap has the form

$$E_n(x) = T(x, a_n) P(x - x_0, b_n) T(x_0, c_n), \quad (10)$$

where $P(x, b)$ and $T(x, a)$ are described by equations (2) and (5) but with general complex parameters, then $E_{n+1}(x)$ has the same form with new parameters a_{n+1} , b_{n+1} , c_{n+1} , and there are recurrent relations between the parameters. We write these relations in a form suitable for calculations, namely

$$\begin{aligned} g &= a_n^{-1} + f_c^{-1}, & b_{n+1} &= z + b_n(1 - zg), \\ h &= gb_{n+1}^{-1}, & a_{n+1}^{-1} &= b_n h, & c_{n+1}^{-1} &= c_n^{-1} + zh. \end{aligned} \quad (11)$$

Let us consider a general set-up with several CRLs installed in the beam path (Fig. 2). To calculate this set-up we begin with the parameters of the incident wave $a_0^{-1} = 0$, $b_0 = z_{oc} + p_1/2$, $c_0^{-1} = 0$, where $p_1 > p$ is the distance corresponding to one chip in the first CRL, and apply the relations (11) for the first chip with γ_1 instead of γ and with $z = p_1$. Then we apply the same relations $(N - 2)$ times for subsequent chips with γ and $z = p_1$. Then we apply the relations for the last chip with γ and $z = p_1/2 + z_1 + p_2/2$ where z_1 is the distance between the first and second CRL and p_2 is the same as p_1 for the second CRL. Then we calculate the second CRL and so on.

As a result, we can obtain numerically the complex parameters a , b , c at the detector which is positioned at some distance from the last CRL. In this approach the intensity of radiation is described by the Gaussian function (Kohn, 2012)

$$I_{ps}(x, x_0) = \frac{z_t}{|b|} \exp\left(-\frac{x_0^2}{2\sigma_0^2}\right) \exp\left(-\frac{(x + Mx_0)^2}{2\sigma^2}\right). \quad (12)$$

The index 'ps' indicates the point source, z_t is a normalization parameter which is equal to the total distance from the source to the end of the last CRL,

$$\sigma = (2K[A - B])^{-1/2}, \quad \sigma_0 = (2K[C - AM])^{-1/2}, \quad (13)$$

where $K = 2\pi/\lambda$ and

$$\begin{aligned} M &= \frac{B}{A - B}, & A &= -\text{Im}(1/a), \\ B &= -\text{Im}(1/b), & C &= -\text{Im}(1/c). \end{aligned} \quad (14)$$

In this work we consider the general case where the centre of the source is shifted from the optical axis (z axis) by the distance x_s . Therefore the density of radiation inside the

source transverse section can be described by the Gaussian function $B_s(x_0 - x_s)$ where

$$B_s(x) = \frac{1}{\sigma_s(2\pi)^{1/2}} \exp\left(-\frac{x^2}{2\sigma_s^2}\right). \quad (15)$$

Here $\sigma_s = w_s/e_2$, $e_2 = (8 \ln 2)^{1/2} = 2.355$ and w_s is the source transverse size (FWHM) along the x axis. We obtain the intensity distribution at the detector taking into account the source size by means of integrating the product of (12) and $B_s(x_0 - x_s)$ over x_0 , namely

$$I_{rs}(x, x_s) = \int dx_0 B_s(x_0 - x_s) I_{ps}(x, x_0). \quad (16)$$

The index 'rs' indicates the real source.

As a result of direct calculations of the integral (16) we obtain

$$I_{rs}(x, x_s) = \frac{S(x_s)}{(2\pi)^{1/2} \sigma_1} \exp\left[-\frac{(x + Mx_s C_s)^2}{2\sigma_1^2}\right], \quad (17)$$

where

$$C_s = \frac{\sigma_0^2}{\sigma_s^2 + \sigma_0^2}, \quad \sigma_1 = (\sigma^2 + M^2 C_s \sigma_s^2)^{1/2}, \quad (18)$$

and $S(x_s)$ is the integral intensity which is described by the equation

$$S(x_s) = (2\pi)^{1/2} \frac{z_t}{|b|} C_s^{1/2} \sigma \exp\left(-\frac{x_s^2 C_s}{2\sigma_0^2}\right). \quad (19)$$

It is of interest to examine how the intensity of radiation depends on the distance in space behind the last CRL. Let us assume now that the parameters a_0 , b_0 , c_0 correspond to the end of the last CRL and z_1 is the distance from this end to the detector (Fig. 3a). The recurrent relation for the parameter b at the detector position in the case of propagation in free space is as follows,

$$b = b_0 + z_1 D, \quad D = (1 - b_0 a_0^{-1}). \quad (20)$$

The effect of beam focusing occurs at the distance $z_1 = z_f$ where the intensity has the maximum value, and therefore the quantity $|b|$ has the minimum value. One can directly verify that the minimum value of $|b|$ is realized at $z_f = -\text{Re}(b_0 D^*)/|D|$. In the general case z_f can be negative (Kohn, 2003). However, this approach is valid only if $z_f > 0$. The important beam parameter is the beam transverse size (BTS), which is the FWHM of the intensity profile. In the case of a point source the BTS is equal to $w = e_2 \sigma$. In reality, taking into account the source size, the BTS is equal to $w_1 = e_2 \sigma_1$. We note that the value w at the focal distance is called the diffraction-limited focus size which is less than the real focus size w_1 .

Since the integral intensity is independent of z_1 , we have the result that the value $G = |b|^2(A - B)$ does not depend on z_1 . On the other hand, the parameter

$$M = \frac{\text{Im}(b)}{G} = \frac{z_1 + Z_1}{z_0 + Z_0}, \quad (21)$$

where

$$\frac{Z_1}{z_0 + Z_0} = \frac{\text{Im}(b_0)}{G}, \quad \frac{1}{z_0 + Z_0} = \frac{\text{Im}(D)}{G}. \quad (22)$$

The parameters Z_0, Z_1 are useful because they equal zero for a single thin lens.

Equations (1)–(22) allow one to examine one long CRL or a system of CRLs with a long distance between them. Such systems have new properties compared with a thin CRL. One is a sensitivity to the orientation of the long CRL, *i.e.* to angular deviations from the optical axis. This angular dependence is described by equation (19). The angle θ is the ratio of the transverse source coordinate x_s and the longitudinal distance z_0 (see Fig. 3a).

We note that a two-dimensional (circular) CRL is described in our approximation by the same equations as the product of intensities for the x and y coordinates (Kohn, 2017). For example,

$$I_{\text{ps}}^{(2)}(x, y, x_0, y_0) = I_{\text{ps}}(x, x_0) I_{\text{ps}}(y, y_0). \quad (23)$$

3. Rocking curve of a long CRL

In the experimental work of Snigireva *et al.* (2004) a two-dimensional (circular) long CRL was investigated. It was composed of $N = 407$ chips. Each chip was a bi-concave Al parabolic lens with $R = 200 \mu\text{m}$, $p = 1 \text{ mm}$ and $d = 15 \mu\text{m}$ (see Fig. 1). The work was performed with the aim of checking the analytical theory of a long CRL (Kohn, 2002, 2003). The longitudinal length of such a CRL was $L = 40.7 \text{ cm}$, the photon energy was 25 keV and the experiment was performed at the ESRF (beamline BM5). The source-to-CRL distance was $z_0 = 40 \text{ m}$. The transverse source size (FWHM) was $80 \mu\text{m}$ vertically and $250 \mu\text{m}$ horizontally.

Among the other properties of the CRL a rocking curve was measured by means of measuring the integral intensity as a function of the angle between the CRL axis and the optical axis. The analytical theory (Kohn, 2002, 2003) did not consider this property. The experimental scans were performed in both planes (x, z) and (y, z) . Both scans were identical to each other. They had the shape of a Gaussian function with a FWHM of approximately 0.40 mrad.

It is problematic to calculate the rocking curve of a long CRL accurately. A rough estimation of the rocking curve FWHM can be obtained in a geometrical optics approximation from the effective aperture of the CRL A_e and the longitudinal length L as $w_\theta^{(g)} = 2A_e/L$. It was shown by Kohn (2017) that $A_e = (\lambda f/2\gamma)^{1/2}$ in the thin-lens approximation, and $f = R_0/2\delta$, $R_0 = R/N$. The parameters δ and β can be obtained by means of an online internet program (Kohn, 2013) as $\delta = 8.645 \times 10^{-7}$, $\beta = 1.760 \times 10^{-9}$.

This program uses the DABAX (2017) data for taking into account the dispersion corrections due to photoelectron absorption of X-rays in matter. In addition, the absorption correction due to the Compton scattering in β was calculated by means of the interpolation equations given by Van Greken & Markowicz (2001). As a result we obtain $A_e = 58.8 \mu\text{m}$ and

$w_\theta^{(g)} = 0.29 \text{ mrad}$. This estimation is smaller than the experimental value of 0.40 mrad.

The equations of the preceding section can be used for calculating the FWHM of the rocking curve in a more accurate approximation. The rocking curve is described by the integral intensity equation (19). In our approach the CRL is oriented along the optical axis but the centre of the source can be shifted from the optical axis. As a result, the direction from the source to the CRL makes the angle $\theta = x_s/z_0$ with the optical axis (see Fig. 3a).

As follows from equation (19), the theoretical rocking curve has a Gaussian shape with FWHM $w_\theta = e_2\sigma_0/(z_0C_s^{1/2})$. We inputted the parameters of the experiment into an online computer program (Kohn, 2018) and obtained $w_\theta = 0.401 \text{ mrad}$ in both the vertical direction and the horizontal direction. We note that the online computer program (Kohn, 2018) is also a result of this work. We have found that the dependence on the source size is very weak and theoretical values coincide with the experimental results quite well. Fig. 3(b) shows a comparison of the experimental data from the work of Snigireva *et al.* (2004) as markers and the theoretical curve of this work as a solid line. The normalized values are shown. In this calculation we assumed a large angular divergence of the beam.

Thus we can conclude that the geometrical optics and the thin-lens approximations are not valid in this case. The rocking curve FWHM becomes larger because ray trajectories inside the CRL are not straight lines. For the same reason the online program gives a CRL effective aperture value $A_e = 74.0 \mu\text{m}$ as an integral relative intensity behind the CRL (Kohn, 2017). We can conclude that accurate calculation on the basis of recurrent relations allows one to obtain the correct rocking curve FWHM in correspondence with the experimental results.

It is of interest that w_θ depends slightly on distance z_0 for large distances. For example, for the distance $z_0 = 400 \text{ m}$ the program gives the values $w_\theta = 0.399 \text{ mrad}$ ($A_e = 73.6 \mu\text{m}$) which is only slightly less compared with the case of $z_0 = 40 \text{ m}$. The reason for this dependence is as follows. The true rocking curve is determined for the plane wave. We calculate the sum of w_θ and the effective angular divergence of the beam α_e . The value of α_e is determined as a ratio of the effective aperture and z_0 . For larger values of z_0 we have smaller values of α_e .

The approach developed in the preceding section allows one to calculate the properties of a system consisting of several CRLs with a relatively large distance between them. Let us consider a system of two CRLs. Each of them has three chips with the same parameters as in the case above and a distance 40.1 cm between them. Therefore the total length of this system is 40.7 cm which is the same as in the case of the experiment but the total number of chips is 6 instead of 407. The focus distance of such a system is 20.2 m, which is much greater than the 0.13 m for the case considered in the experiment.

For such a system and for $z_0 = 40 \text{ m}$ the program gives $w_\theta = 1.792 \text{ mrad}$, $A_e = 389.4 \mu\text{m}$, $w_\theta^{(g)} = 1.913 \text{ mrad}$. For $z_0 = 400 \text{ m}$ the program gives $w_\theta = 1.783 \text{ mrad}$, $A_e = 387.7 \mu\text{m}$, $w_\theta^{(g)} =$

1.905 mrad. Thus we see that for the system of two thin CRLs a correspondence between a geometrical estimation and the program calculation is better even despite the fact that the effective aperture is not well defined in this case.

4. Spatial coherence properties of a long CRL

Coherence is an opportunity to observe the interference fringes. Spatial coherence is an opportunity to create the interference pattern for two points in the transverse section of the beam. One can use Young's experimental setup for measuring the transverse coherent length where an interferometer with two slits is used (Fig. 4). In this case the electric field at the detector is defined by

$$E(x, x_0) = \int dx_i P(x - x_i, z) T_i(x_i) E_0(x_i, x_0), \quad (24)$$

where z is the interferometer-to-detector distance, $T_i(x_i)$ is the transmission function of the interferometer and $E_0(x_i, x_0)$ is the electric field in front of the interferometer. The latter function depends on the coordinate x_0 of the point at the source as described above. We note that the source size is the origin of the decrease in the coherence length.

In the case of a long CRL the function $E_0(x_i, x_0)$ is determined by equation (10). For a large distance z we can choose approximately the function $T_i(x_i)$ in the form

$$T_i(x_i) = \delta(x_i - x_1 + s) + \delta(x_i - x_1 - s), \quad (25)$$

where $\delta(x)$ is the Dirac delta function, x_1 is a shift of the interferometer centre from the optical axis, $s = d/2$ and d is the distance between the slits (Fig. 4). Taking this into account we can write the intensity of radiation at the detector with a normalization factor as above,

$$I_{ps}(x, x_0) = \lambda z_t [I_1(x) + I_2(x)] \quad (26)$$

where

$$I_1(x) = |E_1(-1, x)|^2 + |E_1(1, x)|^2, \quad (27)$$

$$I_2(x) = 2\text{Re}[E_1(-1, x) E_1^*(1, x)], \quad (28)$$

$$E_1(n, x) = P(x - x_1 - ns, z) E_0(x_1 + ns, x_0). \quad (29)$$

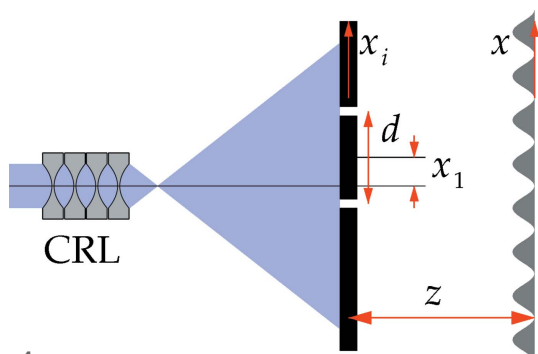


Figure 4
Scheme showing a way to measure and to calculate the transverse coherence length from the definition based on Young's experiment with the interferometer having two slits.

The next step is integrating equation (26) over the coordinate x_0 as described in equation (16). We will assume here that $x_s = 0$. Taking into account equations (17)–(19) we have

$$\int dx_0 B_s(x_0) |E_1(n, x)|^2 = \frac{z_t C_s^{1/2} \sigma}{\lambda z |b| \sigma_1} \exp\left[-\frac{(x_1 + ns)^2}{2\sigma_1^2}\right]. \quad (30)$$

The interference term $I_2(x)$ can be integrated similarly by means of the table integral

$$\int dx \exp(i\beta x + i\gamma x^2) = \left(\frac{i\pi}{\gamma}\right)^{1/2} \exp\left(-i\frac{\beta^2}{4\gamma}\right). \quad (31)$$

We omit calculations and write the result as follows,

$$I_{rs}(x) = I_0(s, x_1) \left\{ 1 + F(s, x_1) \cos\left[2\pi \frac{d}{\lambda z} (x - x_1')\right] \right\} \quad (32)$$

where

$$I_0(s, x_1) = \frac{2z_t C_s^{1/2} \sigma}{\lambda z |b| \sigma_1} \exp\left(-\frac{x_1^2 + s^2}{2\sigma_1^2}\right) \cosh\left(\frac{dx_1}{2\sigma_1^2}\right), \quad (33)$$

$$F(s, x_1) = \exp\left(-\frac{s^2}{2\sigma_1^2} C_1^2\right) \cosh^{-1}\left(\frac{dx_1}{2\sigma_1^2}\right), \quad (34)$$

$$C_1 = \frac{4\pi\sigma_s\sigma}{\lambda|b|} C_s^{1/2}, \quad x_1' = x_1 \left[1 - \frac{z}{z_a} + \frac{z}{z_b} \left(1 - \frac{MC_s\sigma_s^2}{\sigma_1^2} \right) \right]. \quad (35)$$

Here,

$$\frac{1}{z_a} = \text{Re } a^{-1}, \quad \frac{1}{z_b} = \text{Re } b^{-1}, \quad \cosh(x) = \frac{\exp(x) + \exp(-x)}{2}. \quad (36)$$

Since the complex parameters a, b, c are calculated numerically by means of the recurrence equations (11) in the general case, these equations allow one to simplify the calculations only. Nevertheless, some conclusions can be made analytically. The period of the interference fringes is equal to $p = \lambda z/d$. The amplitude of the oscillations depends on the distance d between the slits and the shift x_1 of the interferometer centre position relative to the optical axis. The latter occurs due to the finite width of the beam which can be focused by the CRL.

We define the transverse coherence length $L_{tc}(x_1)$ as the FWHM of the curve $F(s, x_1)$ of equation (34) as a function of the first argument s . This value still depends on the shift of the interferometer. Full dependence $L_{tc}(x_1)$ can be obtained numerically. The particular value for $x_1 = 0$ is equal to

$$L_{tc}(0) = e_2 \frac{\sigma_1}{C_1} = C_0 \frac{\lambda|b|}{w_s} \frac{(\sigma^2 + \sigma_s^2 M^2 C_s)^{1/2}}{\sigma C_s^{1/2}}. \quad (37)$$

Here $C_0 = e_2^2/4\pi = e_1^2 = 0.4413$. We note that an advantage of our approach is the possibility to obtain the analytical equation for the transverse coherence length in the case of a complex set of long CRLs. This is impossible in the general theory of coherence (Mandel & Wolf, 1995).

Let us consider first a most simple case when the CRL is absent. Then $b = z_{0c} = z_0(1 + i\gamma_r)^{-1}$, where $\gamma_r = \sigma_r/z_0$, i.e. equation (3). We note that in the general case $\gamma_r \ll 1$. For

example, typical values for ESRF SR are: $\lambda = 10^{-10}$ m, $\alpha_0 = 10^{-5}$, $z_0 = 44$ m and $\gamma_r = 0.01$. In this case $A = C = \sigma_0^{-1} = 0$, $C_s = 1$, $B = -\gamma_r/z_0$, $|b| \simeq z_0$, and finally

$$L_{tc} = C_0 \frac{\lambda}{\alpha} \left(1 + \frac{w_s^2}{w^2} \right)^{1/2}, \quad (38)$$

where $\alpha = w_s/z_0$, $w = e_2\sigma = z_0\alpha_0$. If the angular divergence of the beam is large and $w \gg w_s$, then we have the well known expression $L_{tc} = C_0\lambda/\alpha$ which is often used with the approximate value of the coefficient $C_0 = 0.5$ (Buffiere & Baruchel, 2015). In this case L_{tc} depends weakly on x_1 . We note that various authors used different definitions for the transverse coherence length and the source size. In terms of the distance d we can write $L_{tc} = e_2\sigma_{tc}/2$. Then $\sigma_{tc} = \lambda z_0/(2\pi\sigma_s)$ (Yabashi *et al.*, 2001). If one defines the source size as $w'_s = 2^{3/2}\sigma_s$ then $\sigma_{tc} = (2^{1/2}/\pi)\lambda z_0/w'_s$ (Kohn *et al.*, 2000). It is of interest that the factor $2^{1/2}/\pi = 0.4501$ is very close to C_0 .

For our example, at the ESRF $w = 440$ μm while the vertical source size w_s is less than 50 μm . However, the horizontal source size may be comparable with this value. Equation (38) may be written in a more clear form as follows,

$$L_{tc} = C_0\lambda \left(\frac{1}{\alpha^2} + \frac{1}{\alpha_0^2} \right)^{1/2}. \quad (39)$$

If the angular divergence of the beam is large, then L_{tc} is determined by the angular size of the source. In the opposite case it is determined by the angular divergence of the beam. Therefore even a point source has a finite spatial coherence length. The reason for this is the finite transverse size of the beam. The condition of a fully coherent beam is formulated as the equality of the beam size $z_0\alpha_0$ and L_{tc} . In the case $\alpha_0 \gg \alpha$ this condition can be formulated as a condition for the transverse emittance $\varepsilon = w_s\alpha_0$ in the form $\varepsilon = C_0\lambda$. In the opposite case we obtain the value for $\alpha_0 = (C_0\lambda/z_0)^{1/2}$ which depends on z_0 . In reality the beam angular divergence is independent of z_0 , and therefore $z_0 = C_0\lambda/\alpha_0^2$. With $\alpha_0 = 10^{-5}$ we obtain $z_0 = 0.5$ m, *i.e.* a very small value. Distances much smaller 30 m are impossible for experiments.

Let us consider now a more complex case of one thin lens under the conditions of most interest, namely, $\gamma_r \ll 1$, $\gamma_1 \ll 1$ and $f \ll z_0$. We have from the recurrent relations (11)

$$b \simeq z_g + i(z_2\gamma_2 - z_0\gamma_r), \quad (40)$$

where

$$z_g = z_0 + z_1 - z_2, \quad z_2 = \frac{z_0 z_1}{f}, \quad \gamma_2 = \gamma_1 + \gamma_r. \quad (41)$$

Equations for any distance z_1 are rather complicated, and therefore we restrict ourselves to the case of the focal length when $z_g = 0$. In this case $z_1 = f(1 - f/z_0)^{-1} \simeq f$.

Below, to simplify the derivations, we will consider rough estimations only. Accurate values can be obtained numerically by means of an online computer program (Kohn, 2018). Therefore $z_2 \simeq z_0$ and $b = iz_0\gamma_1$. Then $B = (z_0\gamma_1)^{-1}$. In the same approximation we calculate $A = (f\gamma_1)^{-1}$, $C = B$. The magnification factor $M \simeq B/A = f/z_0$ while $\sigma_0^{-1} = 0$, $C_s = 1$. Finally, we obtain from (37),

$$L_{tc}(0) = \frac{w_f/w_b}{w'_s}, \quad w'_s = Mw_s, \quad (42)$$

where

$$w_f = (C_0\lambda f\gamma_1)^{1/2}, \quad w_b = \left[w_f^2 + (w'_s)^2 \right]^{1/2}. \quad (43)$$

We note that $w_b = w_1 = e_2\sigma_1$ is the beam size (FWHM) at the focus distance according to (17) and (18), and w_f is the same for a point source (Kohn, 2012).

The first result which follows from equation (42) is the fact that the symmetric coherence length is very large for a point source and is independent of the initial beam angular divergence. The latter follows from the condition $\gamma_r \ll 1$. However, this is not the case for a shifted interferometer. The interference fringes will disappear if $|x_1| > w_f^2/d$ even in the case of a point source. The second result is that, for a source of very large size, $L_{tc}(0) = w_f$, and it is independent of the source size. This value is equal to the diffraction-limited focus size which can be much smaller than the beam size at the focus $w_b \simeq w'_s \gg w_f$. This value depends weakly on the interferometer shift if $|x_1| < w_b^2/d$.

In the general case it is of interest to compare $L_{tc}(0) = L_{tc}^{(1)}$ with $L_{tc}(s) = L_{tc}^{(2)}$. The second value corresponds to the case when one of two slits of the interferometer is located on the optical axis. It follows from equation (34) that in both cases we can write $L_{tc}^{(n)} = 2\sigma_1(\ln X_n)^{1/2}$ where X_n is a solution of the following equations,

$$X_1^H = 2, \quad X_2^H(X_2 + X_2^{-1}) = 4, \quad H = C_1^2/2. \quad (44)$$

The first equation has the analytical solution (37) while the second equation can be calculated numerically. We note that H depends on the source size according to equation (35). It equals zero for the point source and can be quite large for the real source.

In the case of a large source size $H \gg 1$ and we can write $X_n = 1 + g_n$, $g_n \ll 1$. Taking into account the first term of the Taylor series only inside the round brackets we obtain $X_2 \simeq X_1 \simeq 1 + \ln 2/H$ and $L_{tc}^{(2)} \simeq L_{tc}^{(1)} = w_1/C_1 \ll w_1$. In the opposite case $H \ll 1$ it is evident that X_1 is very large and increases to infinity when H decreases to zero, but X_2 remains finite and slightly less than 4. In this case $L_{tc}^{(2)}$ is slightly less than $w_1 \simeq w$.

5. Numerical example

The method using the recurrence relations (11) and the equations presented above allow us to elaborate the computer program for calculating all the main parameters of the X-ray beam, namely the maximum value of the relative intensity, the beam size (FWHM), the width (FWHM) of the rocking curve, the integral intensity, the effective aperture, the magnification factor and the focal length for any value of source transverse size as well as the two lengths of transverse coherence as described at the end of the preceding section.

This program is written in the Javascript programming language with the possibility of working online (Kohn, 2018),

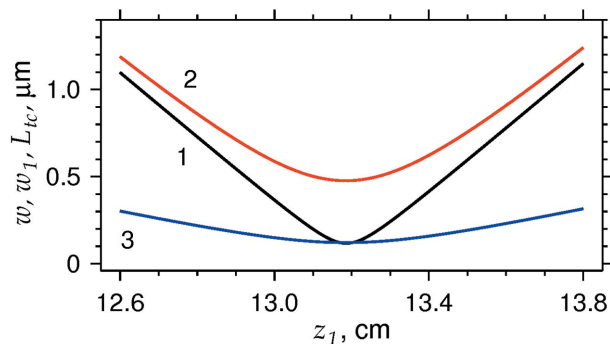


Figure 5 Distance dependence of the beam size for a point source (black curve 1), for a real source (red curve 2) and a transverse coherence length (blue curve 3). See text for details.

thus allowing its use directly on any computer device (laptop, tablet, smartphone). Unfortunately, this format is unable to read and write files. Instead, a data exchange can be performed using the copy-and-paste technique. The program can calculate the distance dependence of the main beam parameters. As an example of the program use, Fig. 5 shows the distance dependence of the beam size for a point source (black curve number 1), the same for a real source (red curve 2) and $L_{tc}^{(1)}$ (blue curve 3) inside the interval close to the focal length.

The results correspond to the case of the long CRL considered in §3, which consists of 407 bi-concave chips made from Al with a curvature radius of 200 μm , aperture 900 μm , source-to-CRL distance $z_0 = 40$ m and source size 50 μm . The energy of the X-ray photons is 25 keV. The focal length counted from the end of the CRL is equal to 13.19 cm. Since the integral intensity $S = e_3 I_m w$ is independent of the distance, the distance dependence of I_m can be obtained as $S/(e_3 w)$. Here $e_3 = (2\pi)^{1/2}/e_2 = 1.064$. We note that, in the case under consideration, $L_{tc}^{(2)} \simeq L_{tc}^{(1)}$.

The main conclusion is that the diffraction-limited beam size at the focus is very close to the coherence length. This fact is evident physically and follows from equation (42) when $w_b \gg w_f$. However, it is difficult to derive this conclusion analytically in the general case. The program shows that the coincidence occurs for 500 chips and more when the focal length decreases to zero if it is counted from the end of the CRL. The second conclusion is that the difference between the beam size and the coherent length is minimal just at the focus, and for other distances it is greater and increases with the distance from the focus.

6. Conclusion

We have shown that the semi-analytical theory of a long X-ray compound refractive lens system based on the recurrence relations allows one to calculate the correct width of the rocking curve of a long CRL which coincides with the experiment by Snigireva *et al.* (2004). The recurrence relations are more complicated compared with the analytical equations and a computer is necessary to obtain the results, but the

computing time is small which allows one to obtain an estimation of the long CRL properties quickly.

In addition, some conclusions can be made without computing. This approach allows us to derive the equations for the transverse coherence length of the beam passing a set of CRLs of arbitrary complexity. We note that it is very difficult in the frame of the Shell-model approach based on the propagation of the mutual coherence function. We are sure that the model of the synchrotron radiation source as a set of independent point radiators is working and truly describes the experimental data.

References

- Afanas'ev, A. M. & Kon, V. G. (1977). *Sov. Phys. Crystallogr.* **22**, 355.
- Bosak, A., Snigireva, I., Napolskii, K. S. & Snigirev, A. (2010). *Adv. Mater.* **22**, 3256–3259.
- Buffiere, J.-Y. & Baruchel, J. (2015). *Synchrotron Radiation. Basics, Methods and Applications*, edited by S. Mobilio, F. Boscherini and C. Meneghini, pp. 389–408. Berlin: Springer.
- DABAX (2017). *ESRF Anonymous FTP Server*, <http://ftp.esrf.eu/pub/scisoft/xop2.3/DabaxFiles/>.
- ESRF-EBS (2017). <https://www.esrf.eu/home/UsersAndScience/Accelerators/ebs---extremely-brilliant-source/ebs-parameters.html>.
- Kohn, V. G. (2002). *JETP Lett.* **76**, 600–603.
- Kohn, V. G. (2003). *J. Exp. Theor. Phys.* **97**, 204–215.
- Kohn, V. G. (2009a). *Poverchnost (Moscow)*, **5**, 32–39.
- Kohn, V. G. (2009b). *J. Surface Investig.* **3**, 358–364.
- Kohn, V. G. (2012). *J. Synchrotron Rad.* **19**, 84–92.
- Kohn, V. G. (2013). *Refraction index*, <http://xray-optics.ucoz.ru/js-pro/cir-pro.htm>.
- Kohn, V. G. (2017). *J. Synchrotron Rad.* **24**, 609–614.
- Kohn, V. G. (2018). *X-ray CRL parameters*, <http://kohnvict.ucoz.ru/jsp/1-crlpar.htm>.
- Kohn, V., Snigireva, I. & Snigirev, A. (2000). *Phys. Rev. Lett.* **85**, 2745–2748.
- Kohn, V., Snigireva, I. & Snigirev, A. (2001). *Opt. Commun.* **198**, 293–309.
- Kohn, V., Snigireva, I. & Snigirev, A. (2003). *Opt. Commun.* **216**, 247–260.
- Lengeler, B. (2010) http://www.esrf.eu/files/live/sites/www/files/Instrumentation/friday-lectures-slides/B-Lengeler_july2010.pdf.
- Mandel, L. & Wolf, E. (1995). *Optical Coherence and Quantum Optics*. New York: Cambridge University Press.
- Ohishi, Y., Baron, A. Q. R., Ishii, M., Ishikawa, T. & Shimomura, O. (2001). *Nucl. Instrum. Methods Phys. Res. A*, **467–468**, 962–965.
- Pereira, N. R., Dufresne, E. M., Clarke, R. & Arms, D. A. (2004). *Rev. Sci. Instrum.* **75**, 37–41.
- Schroer, C. G., Kuhlmann, M., Lengeler, B., Gunzler, T. F., Kurapova, O., Benner, B., Rau, C., Simionovici, A. S., Snigirev, A. A. & Snigireva, I. (2002). *Proc. SPIE*, **4783**, 10–18.
- Singer, A. & Vartanyants, I. A. (2014). *J. Synchrotron Rad.* **21**, 5–15.
- Snigirev, A., Kohn, V., Snigireva, I. & Lengeler, B. (1996). *Nature (London)*, **384**, 49–51.
- Snigirev, A., Kohn, V., Snigireva, I., Souvorov, A. & Lengeler, B. (1998). *Appl. Opt.* **37**, 653–662.
- Snigireva, I., Bosak, A., Snigirev, A., McNulty, I., Eyberger, C. & Lai, B. (2011). *AIP Conf. Proc.* **1365**, 289–292.
- Snigireva, I. I., Kohn, V. G. & Snigirev, A. A. (2004). *Proc. SPIE*, **5539**, 218–225.
- Van Greken, R. & Markowicz, A. (2001). *Handbook of X-ray Spectrometry*, p. 1016. New York: CRC Press.
- Yabashi, M., Tamasaku, K. & Ishikawa, T. (2001). *Phys. Rev. Lett.* **87**, 140801.